Science of the Total Environment 640–641 (2018) 591–598

Contents lists available at ScienceDirect

Science of the Total Environment

journal homepage: www.elsevier.com/locate/scitotenv

Iron(III) minerals and anthraquinone-2,6-disulfonate (AQDS) synergistically enhance bioreduction of hexavalent chromium by *Shewanella oneidensis* MR-1

Ying Meng [a], Ziwang Zhao [a,b], William D. Burgos [c], Yuan Li [a], Bo Zhang [a], Yahua Wang [a,b], Wenbin Liu [a,b], Lujing Sun [a,b], Leiming Lin [a,b], Fubo Luan [a,b,*]

[a] Key Laboratory of Drinking Water Science and Technology, Research Center for Eco-Environmental Sciences, Chinese Academy of Sciences, Beijing 100085, PR China
[b] University of Chinese Academy of Sciences, Beijing 100049, PR China
[c] Department of Civil and Environmental Engineering, The Pennsylvania State University, University Park, PA 16801-1408, United States

HIGHLIGHTS

- Iron(III) minerals alone do not increase the bioreduction rate of Cr(VI).
- Electron shuttle alone increases the bioreduction rate of Cr(VI) by accelerating electron transfer from MR-1 to Cr(VI).
- Iron(III) minerals plus electron shuttle synergistically enhance the bioreduction rate of Cr(VI).

GRAPHICAL ABSTRACT

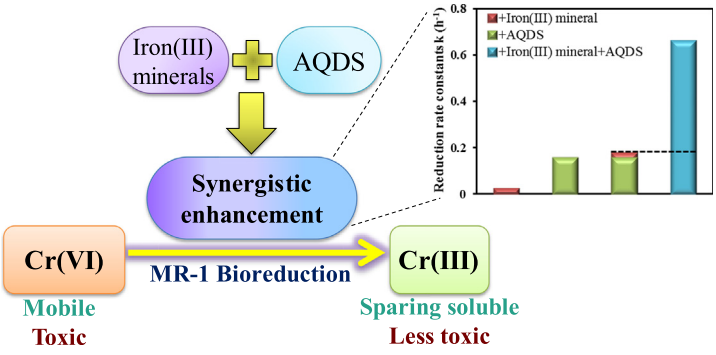

ARTICLE INFO

Article history:
Received 20 March 2018
Received in revised form 25 May 2018
Accepted 26 May 2018
Available online 2 June 2018

Editor: Xinbin Feng

Keywords:
Hexavalent chromium
Iron(III) minerals
Electron shuttle
Bioreduction
Synergistic enhancement

ABSTRACT

Bioreduction of hexavalent chromium (Cr(VI)) to sparingly soluble trivalent chromium (Cr(III)) is a strategy for the remediation of Cr(VI) contaminated sites. However, its application is limited due to the slow bioreduction process. Here we explored the potential synergistic enhancement of iron(III) minerals (nontronite NAu-2, ferrihydrite, and goethite) and electron shuttle anthraquinone-2,6-disulfonate (AQDS) on the bioreduction of Cr(VI) by *Shewanella oneidensis* MR-1. AQDS alone increased the bioreduction rate of Cr(VI) by accelerating electron transfer from MR-1 to Cr(VI). Iron minerals alone did not increase the bioreduction rate of Cr(VI), where the electron transfer from MR-1 to Fe(III) minerals was inhibited due to the toxicity of Cr(VI) to MR-1. AQDS plus NAu-2 or ferrihydrite significantly enhanced the bioreduction rate of Cr(VI) as compared to AQDS or NAu-2/ferrihydrite alone, demonstrating that AQDS plus NAu-2/ferrihydrite had the synergistic effect on bioreduction of Cr(VI). Synergy factor ($k_{cells+Fe+AQDS}/(k_{cells+Fe} + k_{cells+AQDS})$) was used to quantify the synergistic effect of AQDS and iron minerals on the bioreduction of Cr(VI). The synergy factors of AQDS plus NAu-2 were 2.09–4.63 (three Cr(VI) spikes), and the synergy factors of AQDS plus ferrihydrite were 1.89–4.61 (two Cr(VI) spikes). In the presence of Cr(VI), AQDS served as the electron shuttle between MR-1 and iron minerals, facilitating the reduction of Fe(III) minerals to Fe(II). The synergistic enhancement of AQDS and NAu-2/ferrihydrite was attributed to the

* Corresponding author at: Key Laboratory of Drinking Water Science and Technology, Research Center for Eco-Environmental Sciences, Chinese Academy of Sciences, Beijing 100085, PR China.
E-mail address: fbluan@rcees.ac.cn (F. Luan).

https://doi.org/10.1016/j.scitotenv.2018.05.331

generated Fe(II), which could quickly reduce Cr(VI) to Cr(III). Our results provide an attractive strategy to strengthen the bio-immobilization of Cr(VI) at iron-rich contaminated sites through the synergistic enhancement of iron(III) minerals and electron shuttle.

1. Introduction

Chromium is widely used in industry, such as metal plating and alloying, leather tanning, textile manufacturing, paint and pigments, and wood preservatives. A wide range of Cr(VI) concentrations up to 1.8 mM has been found in groundwater due to the widespread industrial use. (Farmer et al., 2002; Gonzalez et al., 2005; Izbicki et al., 2012; Mukhopadhyay et al., 2007; Panagiotakis et al., 2015). Cr(VI) is considered a priority pollutant in the United States and many other countries due to the carcinogenic effect (Saha et al., 2011).

Reduction of toxic Cr(VI) to sparingly soluble, less toxic Cr(III) has been proven to be successful for in-situ remediation of Cr(VI) contaminated groundwater and soil (Hori et al., 2015; Wielinga et al., 2001). Cr(VI) can be reduced biotically by several types of Cr(VI)-tolerant microorganisms (Sathishkumar et al., 2017; Tahri Joutey et al., 2014; Zheng et al., 2015), and abiotically by aqueous or structural Fe(II) from reduced iron minerals (Bishop et al., 2014; Buerge and Hug, 1997; Døssing et al., 2011; Pettine et al., 1998; Sedlak and Chan, 1997). The direct bioreduction of Cr(VI) is a slow process, several orders of magnitude slower than the abiotic reduction by Fe(II) (Nyman et al., 2002). Fe(III) minerals (such as iron oxides and Fe-bearing clay minerals) are ubiquitous in groundwater and soil. Alternatively, dissimilatory metal-reducing bacteria (DMRB) can reduce a variety of Fe(III) minerals to aqueous/structural Fe(II) (Luan et al., 2010; Luan et al., 2015). Bioreduction of Fe(III) minerals by DMRB to produce biogenic Fe(II) has been proposed as a promising approach to promote Cr(VI) reduction. However, the bioreduction of Fe(III) minerals by DMRB is usually inhibited by Cr(VI) due to the toxicity of Cr(VI) (Nyman et al., 2002).

Electron shuttles such as quinones and humic substances may help overcome the inhibition of Fe(III) minerals -mediated Cr(VI) reduction. Electron shuttles significantly enhanced the bioreduction rate of various Fe(III) minerals by DMRB (Brookshaw et al., 2014; Luan et al., 2014; O'Loughlin, 2008). Although the bioreduction of Fe(III) minerals by DMRB was inhibited by Cr(VI) (Viamajala et al., 2003), the electron transfer from DMRB to Fe(III) minerals via electron shuttles may facilitate the reduction of Fe(III) minerals, and hence significantly facilitate the reduction rate of Cr(VI). We hypothesized that the combined effect of iron minerals and electron shuttles would synergistically promote the bioreduction of Cr(VI). Such knowledge is particularly important for developing high-efficiency method for the remediation of Cr(VI) contaminated aquifers.

In the current work, we examined the potential synergistic enhancement of Fe(III) minerals and the electron shuttle on the bioreduction of Cr(VI) by the DMRB. Iron-bearing clay minerals and iron(oxyhydr)oxides are the most abundant iron mineral phase in the natural environment. An iron-bearing clay mineral (nontronite NAu-2) and the iron (oxyhydr)oxides (ferrihydrite and goethite) were selected for this study. Nontronite NAu-2 is a model iron-bearing clay mineral which has been widely used in previous studies (Bishop et al., 2014; Luan et al., 2015). Ferrihydrite and goethite present poorly and well crystalline iron (oxyhydr)oxides, respectively. The bioreduction of Nontronite NAu-2 yields structure Fe(II) (Neumann et al., 2011), while the bioreduction of ferrihydrite and goethite yields aqueous or surface-associated Fe(II) (Gorski and Scherer, 2011). AQDS was chosen as the model electron shuttle because it has been used extensively for stimulating the redox reactions involved in contaminant transformation (Fredrickson et al., 2000; O'Loughlin, 2008). *Shewanella oneidensis* MR-1 was chosen as the model DMRB since it has been studied intensively in terms of the bioreduction of heavy metals (such as uranium, chromium, and vanadium) (Myers et al., 2004; Sani et al., 2008; Viamajala et al., 2003). Experiments were designed to study the bioreduction of Cr(VI) by DMRB in the presence/absence of iron minerals and AQDS. Cr(VI) was re-spiked into the batch reactors multiple times to evaluate the long-term effects of iron minerals and AQDS on the bioreduction of Cr(VI). Abiotic Cr(VI) reduction experiments were also conducted with biologically reduced and pasteurized Fe(III) minerals to examine the role of biogenic Fe(II) on the reduction of Cr(VI).

2. Materials and methods

2.1. Microorganism and culture conditions

Shewanella oneidensis MR-1(hereafter referred to as MR-1) was cultured aerobically on tryptic soy broth without dextrose (TSB-D). Cells were harvested by centrifugation (3500 RCF, 10 min) and washed three times with anoxic 4-(2-hydroxy-ethyl)-1-piperazineethanesulfonic acid (HEPES) buffer (30 mM, pH 7.0). The cells were resuspended in anoxic HEPES buffer in an anoxic chamber for further use. All experiments were conducted at 25 °C.

2.2. Minerals and chemicals

Nontronite NAu-2 was purchased from The Clay Minerals Society. The composition of NAu-2 has been reported by John L. Keeling (Keeling et al., 2000). NAu-2 was suspended in 0.5 M NaCl for 24 h, then separated by centrifugation, yielding the 0.5–2.0 μm clay size fraction. NAu-2 clay fraction stock solution (20 g L^{-1}) was prepared in anoxic 30 mM HEPES buffer (pH 7.0). The NAu-2 clay fraction contained 4.1 mmol Fe/g clay and 99.4% Fe(III) based on the HF-H_2SO_4/phenanthrolinedigestion method (Luan and Burgos, 2012).

Ferrihydrite ($5FeOOH \cdot 2H_2O$) was synthesized by the titration of Fe $(NO_3)_3 \cdot 9H_2O$(0.2 M) with 1 M KOH to pH 7–8 (Ona-Nguema et al., 2005; Schwertmann and Cornell, 2008). Goethite was prepared following the procedures of Ona-Nguema et al. (Berrodier et al., 2004; Ona-Nguema et al., 2005). Surface areas of ferrihydrite and goethite were determined using BET method, which were 258 and 79 m^2/g, respectively.

Regent grade $K_2Cr_2O_7$ were used to prepare 8.0 mM (spike I) and 40 mM (spike II and spike IIII) stock solution in anoxic deionized water.

2.3. Bioreduction of Cr(VI) in the presence of Fe(III) minerals and AQDS

Batch experiments were conducted in autoclaved serum bottles sealed with thick butyl rubber stoppers. All preparations were performed in an anoxic chamber (<0.1 ppm, O_2) in a 25 °C constant temperature room. Reactors were filled with 20 mL of deoxygenated 30 mM HEPES buffer (pH 7.0) containing various combinations of Cr(VI) (0.8 mM), Fe(III) minerals (2.0 g L^{-1}), AQDS (0.1 mM), and MR-1 (7.0×10^8 cell/mL). Excess sodium lactate (8 mM final conc.) was filter-sterilized as the electron donor for bioreduction experiments. Cr(VI) was re-spiked with 40 mM stock solution into all reactors (0.8 mM final conc.) when Cr(VI) concentrations were <0.01 mM in the reactors containing MR-1, Fe(III) minerals, and AQDS. During spike II and spike III, the addition volume of Cr(VI) was amount to 2% of the total volume. Control reactors were prepared containing Cr(VI), lactate, and HEPES buffer. Other control reactors were filled with MR-1 and iron minerals (NAu-2, ferrihydrite or goethite). Reactors were incubated at 150 rpm on orbital shakers in the anoxic chamber. All experiments were run in duplicate. After cell addition, samples were periodically removed with sterile needle and syringe inside the anoxic chamber.

2.4. Abiotic reduction of Cr(VI) by bioreduced Fe(III) mineral

Abiotic reduction of Cr(VI) was performed with bioreduced NAu-2. Bioreduced NAu-2 was prepared using MR-1 and NAu-2 as described above. Reactors were incubated for about 180 h when the biogenic Fe (II) concentrations stopped increasing. The reactors were pasteurized at 75 °C for 60 min (three times over 5 days) to deactivate biological activity (Luan et al., 2015). Cr(VI) was added to the pasteurized reactors (0.8 mM) and samples were periodically removed with sterile needle and syringe.

2.5. Analytical methods

Aqueous Cr(VI) was qualified by the diphenylcarbazide method using a UV/Vis spectrophotometer at 540 nm (Butler et al., 2015). The bioreduction of ferrihydrite and goethite yields soluble or surface-associated Fe(II). Total Fe(II) (soluble and surface-associated Fe(II)) in ferrihydrite and goethite experiments was measured by 0.5 N HCl method after a 24 h extraction, and then analyzed using the ferrozine assay (Dixit and Hering, 2006; Kukkadapu et al., 2006; Luan et al., 2010). The bioreduction of Nontronite NAu-2 yields structure Fe(II). HCl (0.5 N) method had a low efficiency to extract the structure Fe(II) in clay minerals. Therefore, a modified anoxic HF-H_2SO_4/phenanthroline digestion method was used to measure Fe(II) in NAu-2 experiments (Luan and Burgos, 2012).

2.6. X-ray photoelectron spectroscopy (XPS)

XPS was used to determine the valence state of Cr after bioreduction. At the end of the bioreduction experiments, solid samples were collected by centrifugation and freeze-dried. The XPS analysis was performed using an ESCALAB 250Xi XPS (Thermo Fisher Scientific, USA) with an Al Kα X-ray source over a specific 500 μm area.

2.7. Kinetic analyses

The rate of Cr(VI) reduction was modeled as pseudo-first-order with respect to Cr(VI) concentration according to

$$-\frac{d[\mathrm{Cr(VI)}]}{dt} = k \times [\mathrm{Cr(VI)}] \quad (1)$$

where k is the first-order rate constant (h^{-1}); k_{cells} used to denote the first-order rate constant only in the presence of MR-1; $k_{cells+AQDS}$ is used to denote the first-order rate constant in the presence of MR-1 and AQDS; $k_{cells+Fe}$ is used to denote the first-order rate constant in the presence of MR-1 and iron minerals (NAu-2, ferrihydrite or goethite); $k_{cells+Fe+AQDS}$ is used to denote the first-order rate constant in the presence of MR-1, iron minerals, and AQDS. [Cr(VI)] is the concentration of Cr(VI).

To quantitatively compare Cr(VI) reduction rates with and without AQDS/Fe(III) minerals, we defined "AQDS enhancement", "Fe(III) enhancement" and "AQDS + Fe(III) enhancement" as (Luan et al., 2015)

$$\text{AQDS enhancement factor} = \frac{k_{cells+AQDS}}{k_{cells}} \quad (2)$$

$$\text{Fe(III) enhancement factor} = \frac{k_{cells+Fe}}{k_{cells}} \quad (3)$$

$$\text{AQDS + Fe(III) enhancement factor} = \frac{k_{cells+Fe+AQDS}}{k_{cells}} \quad (4)$$

In this study, some of the AQDS+Fe(III) enhancement factors are much higher than the AQDS enhancement factors and Fe(III) enhancement factors, indicating a potential synergistic effect of iron mineral and AQDS on bioreduction of Cr(VI). The synergistic effect is the creation of a whole that is greater than the simple sum of its parts (Wikipedia, 2017 (accessed 10 December 2017)). To quantify the synergistic effect of iron minerals and AQDS on the bioreduction of Cr(VI) by DMRB, synergy factor (SF) was defined as (Weng et al., 2013; Zhou et al., 2011; Zhou et al., 2013)

$$\text{Synergy factor} = \frac{k_{cells+Fe+AQDS}}{k_{cells+Fe} + k_{cells+AQDS}} \quad (5)$$

If SF > 1.0, it means synergistic effect; If synergistic factor ≤ 1.0, it means no synergistic effect.

3. Results and discussion

3.1. Bioreduction of Cr(VI) in the presence of nontronite NAu-2 and AQDS

To test the combined effects of NAu-2 and AQDS on the bioreduction of Cr(VI), MR-1 was used to reduce Cr(VI) in the presence/absence of NAu-2 and AQDS. As expected, MR-1 could reduce Cr(VI) or Fe(III) in NAu-2 when provided as the sole electron acceptor (Fig. 1a,d). After the first spike of Cr(VI), the first-order rate constant for Cr(VI) reduction (k_{cells}) by MR-1 alone was 0.035 ± 0.003 h^{-1}, and increased to 0.191 ± 0.001 h^{-1} in the presence of AQDS ($k_{cells+AQDS}$) (Table 1), confirming that electron shuttles could accelerate the transformation of electrons from MR-1 to Cr(VI) (Field et al., 2013; Liu et al., 2010). The bioreduction rate in the presence of NAu-2 ($k_{cells+NAu\text{-}2}$ = 0.032 ± 0.001 h^{-1}) was almost the same as the rate obtained with MR-1 alone (Table 1), suggesting that NAu-2 had no influence on the bioreduction of Cr(VI). However, $k_{cells+AQDS+NAu\text{-}2}$ increased to 0.467 ± 0.005 h^{-1} in the presence of both NAu-2 and AQDS. The enhancement factors of AQDS, NAu-2 and AQDS+NAu-2 were 5.46 ± 0.01, 0.90 ± 0.01 and 13.33 ± 0.14, respectively (Table 2). Much more enhancement of Cr (VI) bioreduction was achieved in the presence of both NAu-2 and AQDS than that of NAu-2 or AQDS alone (Fig. 2a, Table 2), suggesting a potential synergistic enhancement of NAu-2 and AQDS on bioreduction of Cr(VI). The calculated synergy factor (SF) was 2.09 in the presence of NAu-2 and AQDS (Table 2), which clearly showed that NAu-2 and AQDS had a synergistic effect (SF > 1.0) on bioreduction of Cr(VI). Control vials containing NAu-2 and Cr(VI) did not show a significant decrease in Cr(VI) concentration over the duration of the experiment, indicating that sorption of Cr(VI) on NAu-2 was negligible. X-ray photoelectron spectroscopy (XPS) was used to analyze the valence state of Cr after the bioreduction of Cr(VI). XPS spectrum (Fig. S1) confirmed that the product of bioreduction was Cr(III) no matter in the presence/absence of NAu-2 and AQDS.

Measurement of Fe(II) concentrations over time revealed the role that Fe(II) played in the bioreduction process. The concentration of Fe (II) was <0.5 mM at 25 h in the presence of MR-1, NAu-2, and Cr(VI) (Fig. 1d), which was significantly lower than that in the absence of Cr (VI) (2.4 mM, Fig. 1d). Given that the rates of Cr(VI) reduction with/without NAu-2 were almost same (with NAu-2: 0.032 ± 0.001 h^{-1}; without NAu-2: 0.035 ± 0.001 h^{-1}), it is likely that bioreduction of iron minerals by DMRB was inhibited due to the toxic effect of Cr(VI) (Nyman et al., 2002). However, the concentration of Fe(II) increased to 2.0 mM at 25 h in the presence of AQDS (Fig. 1d), suggesting that AQDS facilitated the bioreduction of NAu-2-Fe(III) in the presence of Cr(VI). Therefore, the synergistic enhancement of NAu-2 and AQDS on bioreduction of Cr(VI) was likely driven by the generated Fe(II), which could promote the abiotic reduction of Cr(VI). To verify this, Cr(VI) was re-spiked into the reactors two additional times (Spike II at t = 25 h and Spike III at t = 50 h) (Fig. 1). For all three spikes, obvious synergistic enhancement of NAu-2 and AQDS on bioreduction of Cr(VI) was observed (Fig. 2). The synergy factors increased with each sequential spike of Cr(VI) (Spike I 2.09, Spike II 4.03, Spike III 4.63, Table 3). The change of Fe(II) concentrations over time confirmed the important role of generated Fe(II) played in the reduction of Cr(VI). In spike II

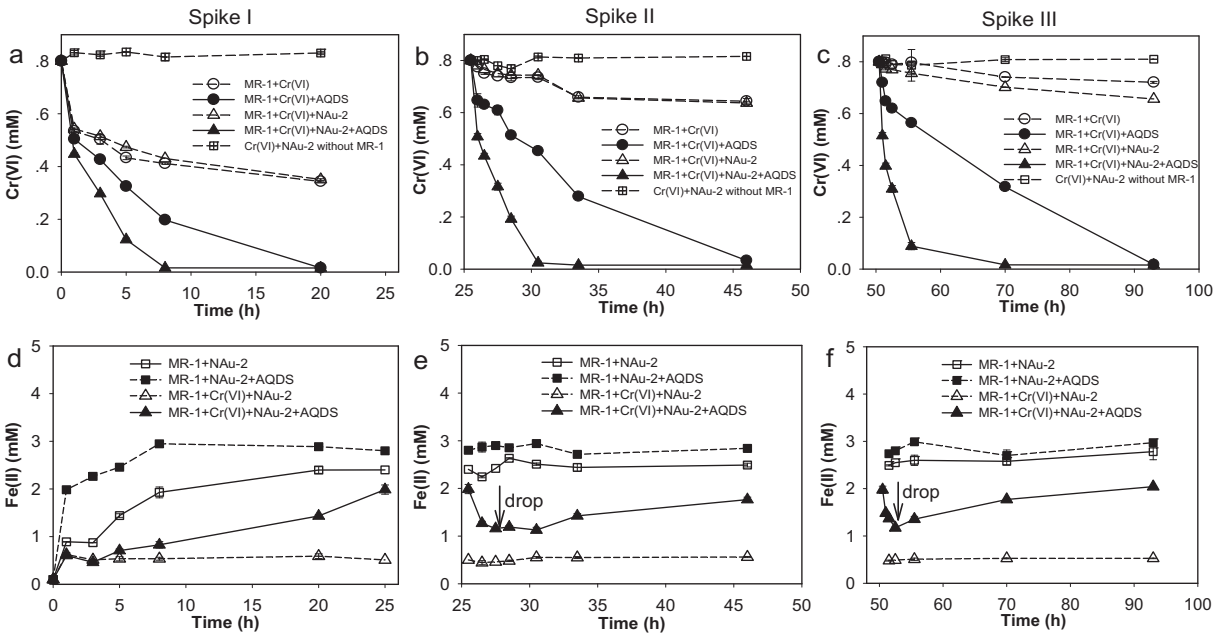

Fig. 1. Biological reduction of Cr(VI) by MR-1 in the presence/absence of NAu-2 and AQDS. Experiments were initiated at $t = 0$ h with 0.8 mM Cr(VI), 7.0×10^8 cells/mL MR-1, and 8.0 mM lactate with/without NAu-2 (2.0 g L^{-1}) and AQDS (0.1 mM) in 30 mM HEPES buffer, pH 7.0. Cr(VI) (0.8 mM) was re-spiked into the reactors at $t = 25$ h and $t = 50$ h. (a–c) Cr(VI) concentrations versus time. (d–f) Fe(II) concentrations versus time.

and spike III, obvious drops of generated Fe(II) were observed with each spike of Cr(VI) (Fig. 1e, f). The drops of generated Fe(II) was attributed to the Cr(VI) reduction by Fe(II) since Cr(VI) was the only oxidant present in the system.

3.2. Bioreduction of Cr(VI) in presence of ferrihydrite/goethite and AQDS

In the natural environment, a large portion of the iron is present as iron(oxyhydr)oxides (Xu et al., 2005). To test the role of iron (oxyhydr)oxides and AQDS played in the process of Cr(VI) reduction, ferrihydrite and goethite were applied to instead of nontronite NAu-2. Ferrihydrite was poorly ordered but had more reactivity and larger specific surface area (Berrodier et al., 2004). In the first spike of Cr(VI) (Spike I in Fig. S3a), the bioreduction kinetics of Cr(VI) in the presence of ferrihydrite displayed biphasic behavior due to the fast adsorption of Cr(VI) by ferrihydrite in the first hour (Fig. S3a). In the first hour, the first-order rate constant for Cr(VI) removal was 1.049 ± 0.002 h^{-1}(Table 1) in the presence of ferrihydrite ($k_{cells+Ferrihydrite}$), which was higher than that by MR-1 alone (0.460 ± 0.022 h^{-1}) due to the sorption of Cr(VI) by ferrihydrite. In the following progress, the first-order rate constants were same in presence/absence of ferrihydrite (0.023 ± 0.001 h^{-1}, 0.023 ± 0.003 h^{-1}). In the re-spiked experiment, the sorption of Cr(VI) on ferrihydrite reached balance, and then ferrihydrite showed a slight influence on the Cr(VI) removal (0.012 ± 0.002 h^{-1} with ferrihydrite versus 0.010 ± 0.001 h^{-1} without ferrihydrite). Only a small amount of Fe(II) (<0.1 mM, Fig. S3e) was observed

Table 1
Summary of first-order rate constants for Cr(VI) reduction with combinations of MR-1, Cr(VI), NAu-2/ferrihydrite/Goethite and AQDS.[a]

Fe(III) minerals	Reaction description	Spike I			Spike II			Spike III		
		Time (h)	k_{red} (h^{-1})[b]	$R^{2,c}$	Time (h)	k_{red} (h^{-1})[b]	$R^{2,c}$	Time (h)	k_{red} (h^{-1})[b]	$R^{2,c}$
NAu-2	MR-1 + Cr(VI)	0–25	0.035 ± 0.003	0.70	25–50	0.011 ± 0.001	0.79	50–93	0.003 ± 0.000	0.92
	MR-1 + Cr(VI) + AQDS	0–25	0.191 ± 0.001	0.99	25–50	0.153 ± 0.006	0.98	50–93	0.086 ± 0.000	0.94
	MR-1 + Cr(VI) + NAu-2	0–25	0.032 ± 0.001	0.71	25–50	0.011 ± 0.000	0.82	50–93	0.004 ± 0.000	0.94
	MR-1 + Cr(VI) + NAu-2 + AQDS	0–25	0.467 ± 0.005	0.96	25–50	0.660 ± 0.050	0.94	50–93	0.416 ± 0.003	0.98
Ferrihydrite	MR-1 + Cr(VI)	0–1[d]	0.460 ± 0.022	1.00	27–42	0.010 ± 0.001	0.83	/	/	/
		1–27	0.023 ± 0.003	0.99						
	MR-1 + Cr(VI) + AQDS	0–1[d]	0.528 ± 0.063	1.00	27–42	0.126 ± 0.001	0.98	/	/	/
		1–27	0.199 ± 0.003	0.99						
	MR-1 + Cr(VI) + Ferrihydrite	0–1[d]	1.049 ± 0.002	1.00	27–42	0.012 ± 0.002	0.79	/	/	/
		1–27	0.023 ± 0.001	0.98						
	MR-1 + Cr(VI) + Ferrihydrite + AQDS	0–1[d]	1.254 ± 0.002	1.00	27–42	0.636 ± 0.060	0.95	/	/	/
		1–27	0.420 ± 0.004	0.99						
Goethite	MR-1 + Cr(VI)	0–25	0.035 ± 0.003	0.70	25–34	0.020 ± 0.002	0.86	/	/	/
	MR-1 + Cr(VI) + AQDS	0–25	0.191 ± 0.001	0.99	25–34	0.117 ± 0.001	0.96	/	/	/
	MR-1 + Cr(VI) + Goethite	0–25	0.030 ± 0.001	0.80	25–34	0.022 ± 0.001	0.88	/	/	/
	MR-1 + Cr(VI) + Goethite + AQDS	0–25	0.187 ± 0.001	0.98	25–34	0.125 ± 0.001	0.94	/	/	/

[a] All experiments conducted with 7.0×10^8 cells mL^{-1} MR-1, 0.8 mM Cr(VI), 2.0 g L^{-1} (+) or 0 (−) iron minerals (NAu-2, ferrihydrite and goethite), 0.1 mM AQDS (+) or 0 (−), and 8 mM lactate as electron donor in 30 mM HEPES, pH 7.0.
[b] The values represent the means ± standard error from duplicate samples.
[c] R^2 for regression of $\ln([Cr]_t/[Cr]_0)$ versus time of spike-period.
[d] The bioreduction kinetics of Cr(VI) in the presence of ferrihydrite displayed biphasic behavior due to the fast adsorption of Cr(VI) by ferrihydrite in the first hour, and then the rate of Cr (VI) reduction was modeled as two phases (0–1 h and 1–27 h).

Table 2
The enhancement factors of AQDS, Fe(III) minerals and AQDS + Fe(III) minerals on bioreduction of Cr(VI).

Fe(III) minerals	Enhancement factors	Spike I		Spike II		Spike III	
		Time (h)	Values	Time (h)	Values	Time (h)	Values
NAu-2	AQDS	0–25	5.46 ± 0.01	25–50	13.86 ± 0.50	50–93	28.53 ± 0.00
	NAu-2	0–25	0.90 ± 0.01	25–50	1.03 ± 0.03	50–93	1.43 ± 0.03
	AQDS + NAu-2	0–25	13.33 ± 0.14	25–50	60.02 ± 4.52	50–93	138.60 ± 10.20
Ferrihydrite	AQDS	0–1	1.15 ± 0.14	27–42	12.55 ± 0.09	/	/
		1–27	8.65 ± 0.13				
	Ferrihydrite	0–1	2.28 ± 0.00	27–42	1.26 ± 0.16	/	/
		1–27	1.00 ± 0.05				
	AQDS + Ferrihydrite	0–1	2.73 ± 0.01	27–42	63.61 ± 6.05	/	/
		1–27	18.25 ± 0.17				
Goethite	AQDS	0–25	5.46 ± 0.01	25–34	5.86 ± 0.04	/	/
	Goethite	0–25	0.86 ± 0.02	25–34	1.09 ± 0.03	/	/
	AQDS + Goethite	0–25	5.33 ± 0.01	25–34	6.26 ± 0.06	/	/

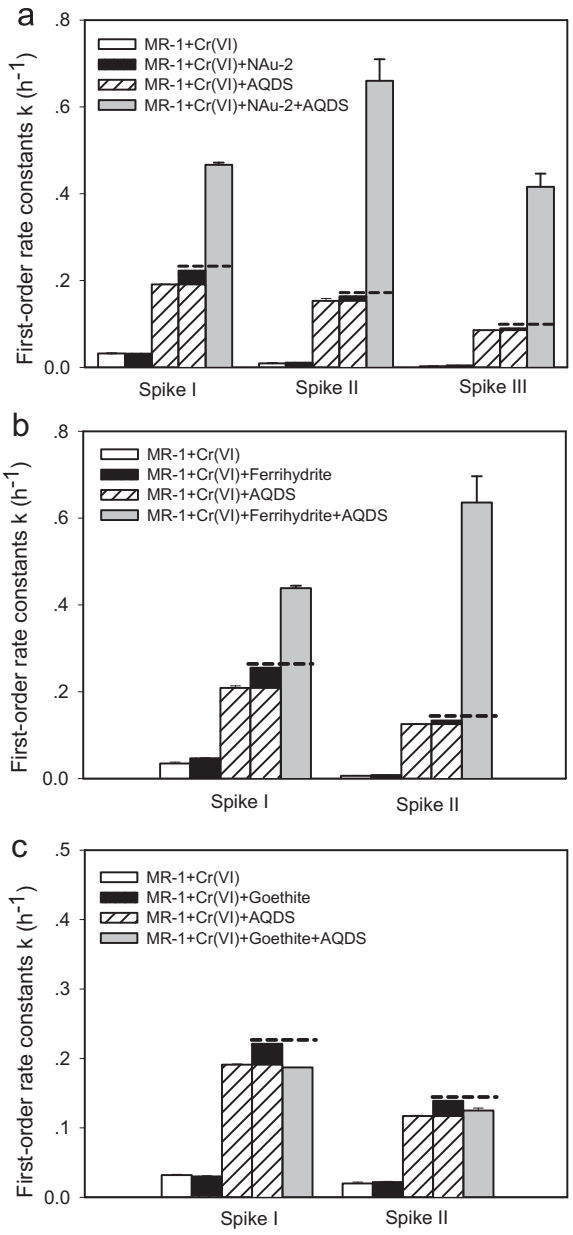

Fig. 2. First-order rate constants for Cr(VI) reduction with combinations of MR-1, Cr(VI), AQDS, and Fe(III) minerals. (a) NAu-2 at three spikes, (b) Ferrihydrite at two spikes, and (c) goethite at two spikes.

in the presence of Cr(VI), confirming that the enhancement of Cr(VI) removal in the first hour (spike I) was due to the sorption of Cr(VI), and was not due to reduction of Cr(VI) by Fe(II). After 1 h, the ferrihydrite enhancement factors were 1.00–1.26, illustrating ferrihydrite also had little effect on bioreduction of Cr(VI) (Table 2). However, in the presence of both ferrihydrite and AQDS, obvious synergistic enhancement on bioreduction of Cr(VI) was observed in the two spikes (Fig. S3b, Table 3). The synergy factors increased with each sequential spike of Cr(VI) (Spike I 1.89, Spike II 4.63, Table 3). Clear drops of Fe(II) from 0.89 mM to 0.09 mM were also observed with spike of Cr(VI) in the presence of both ferrihydrite and AQDS in spike II, which was consistent with the result obtained with NAu-2.

Compared to ferrihydrite, the sorption of Cr(VI) on goethite was negligible (Fig. S4a). Goethite had almost no influence on the bioreduction of Cr(VI) in both spike I and spike II (Spike I: $k_{cells+Goethite} = 0.030 \pm 0.001\ h^{-1}$; $k_{cells} = 0.035 \pm 0.003\ h^{-1}$; Spike II: $k_{cells+Goethite} = 0.022 \pm 0.001\ h^{-1}$; $k_{cells} = 0.020 \pm 0.002\ h^{-1}$, Table 2), which was consistent with the result with NAu-2 and ferrihydrite. The enhancement factors of AQDS and AQDS + goethite were both in the range of 5.33–6.26 for two Cr(VI) spikes. Unlike NAu-2 and ferrihydrite, there was no obvious synergistic effect of goethite and AQDS on bioreduction of Cr(VI) in the two spikes, where the synergy factors were 0.84 and 0.90 in Spike I and Spike II, respectively (Table 3).

3.3. Abiotic reduction of Cr(VI) by biogenic NAu-2-Fe(II)

Abiotic reduction experiment was conducted to further confirm the role of generated Fe(II) on the reduction of Cr(VI). The abiotic reduction of Cr(VI) by biogenic Fe(II) was a fast process, where both Fe(II) and Cr (VI) concentrations decreased sharply at the first sampling point and then decreased slightly (Fig. 3a and b). The abiotic reduction rate of Cr (VI) by Fe(II) was 1.38 mM h^{-1}, which was 28 times faster than the biotic reduction rate by MR-1 (0.05 mM h^{-1}). Therefore, Fe(II) could significantly enhance the bioreduction rate of Cr(VI) by MR-1. Fe(II) concentrations decreased from 2.6 mM to 1.2 mM and remained unchanged after 0.3 h although there was still 0.4 mM Cr(VI) in the reactors. These data indicated that a fraction of biogenic Fe(II) (around 1.2 mM) in NAu-2 was not reactive for the reduction of Cr(VI). These data were consistent with the drops of biogenic Fe(II) in the

Table 3
The synergy factors of iron minerals and AQDS on bioreduction of Cr(VI).

Synergy effect	Spike I		Spike II		Spike III	
	Time (h)	SF	Time (h)	SF	Time (h)	SF
NAu-2 + AQDS	0–25	2.09	25–50	4.03	50–93	4.63
Ferrihydrite + AQDS	0–1	0.80	27–42	4.61	/	/
	1–27	1.89				
Goethite + AQDS	0–25	0.84	25–34	0.90	/	/

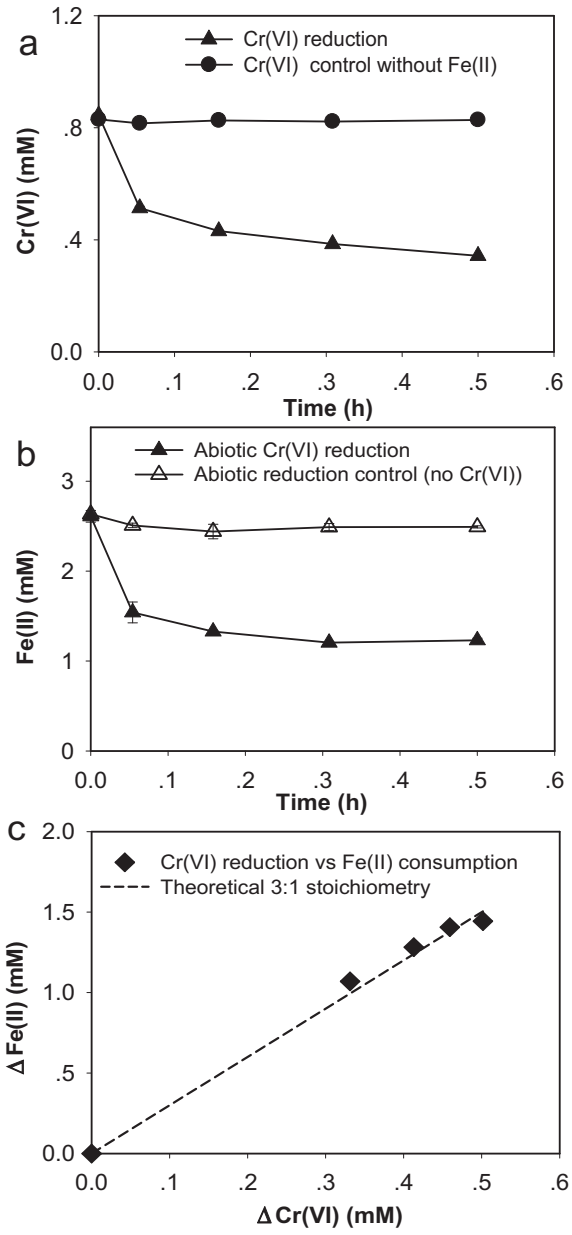

Fig. 3. Abiotic reduction of Cr(VI) by biological reduced structural Fe(II) in NAu-2. (a) Cr (VI) concentrations versus time. (b) Fe(II) concentrations versus time. (c) Stoichiometric relationships between Δ mol Fe(II) and Δ mol Cr(VI). Dashed line represents theoretical stoichiometry of 3 Δ mol Fe(II) to 1 Δ mol Cr(VI).

bioreduction experiments, where biogenic Fe(II) concentrations dropped to 1.1–1.2 mM with each spike of Cr(VI) (Fig. 1e,f). These data were also explained that although a small amount of biogenic Fe (II) (<0.6 mM) was found in all three spikes (Fig. 1d,e,f), NAu-2 did not enhance the bioreduction of Cr(VI) by MR-1 in the absence of AQDS (Fig. S2a,b,c).

In abiotic reduction experiment, a good stoichiometric agreement between 3 mol of ΔFe(II) consumed per 1 mol of ΔCr(VI) reduction (Fig. 3c). These results confirmed that Cr(VI) was reduced to Cr(III). These results also confirmed that the abiotic reduction of Cr(VI) was attributed to the biogenic Fe(II) and was not other reductants.

3.4. Synergistic effect of Fe(III) minerals and AQDS on bioreduction of Cr(VI)

Clear synergistic effects of AQDS and NAu-2/ferrihydrite on the bioreduction of Cr(VI) by DMRB were observed in this study (Fig. 2a,b, Table 3). The synergy factors of NAu-2 plus AQDS and ferrihydrite plus AQDS were 2.09–4.63 and 1.89–4.61, respectively (Table 3). In the presence of DMRB, iron minerals, and electron shuttles in anoxic environments, there are four possible pathways for the reduction of contaminants (Fig. 4): (I) direct bioreduction (Pathway a in Fig. 4); (II) indirect reduction by bioreduced electron shuttles (Pathway b in Fig. 4); (III) indirect reduction by biogenic Fe(II) in the presence of Fe (III) minerals (Pathway c in Fig. 4); and (IV) indirect reduction coupled to both Fe(III) minerals and electron shuttles (Pathway d in Fig. 4). In our previous study, all the four pathways have been confirmed on the bioreduction of nitroaromatic compounds (NACs) (Luan et al., 2010). However, no synergistic effect of Fe(III) minerals and electron shuttles was observed on the bioreduction of NACs by DMRB, where both iron minerals and electron shuttles could enhance the bioreduction of NACs independently (Luan et al., 2010). In this study, MR-1 could reduce Cr(VI) directly (Pathway a in Fig. 4), and AQDS served as the electron shuttle between MR-1 and Cr(VI) (Pathway b in Fig. 4). The bioreduction of all three iron minerals (nontronite NAu-2, ferrihydrite, and goethite) was inhibited by Cr(VI), where the bioreduction rate of Fe(III) in NAu-2 and ferrihydrite were 0.096 ± 0.003 mM h^{-1} and 0.070 ± 0.001 mM h^{-1}, and decreased to 0.020 ± 0.002 mM h^{-1} and 0.003 ± 0.000 mM h^{-1} in the presence of Cr(VI) (Fig. 5). The indirect reduction of Cr(VI) by biogenic Fe(II) (Pathway c in Fig. 4) was infeasible in this study due to insufficient biogenic Fe(II) in the absence of AQDS. Therefore, iron minerals have almost no influence on the bioreduction of Cr(VI) (Fig. 1, Fig. S3, and Fig. S4). However, in the presence of both Cr(VI) and AQDS, the bioreduction rate of Fe(III) in NAu-2 and ferrihydrite increased to 0.080 ± 0.004 mM·h^{-1} and 0.033 ± 0.001 mM h^{-1} (Fig. 5). These data implied that AQDS served as the electron shuttle between MR-1 and NAu-2/ferrihydrite even in the presence of Cr(VI), which facilitated the reduction of Fe(III) minerals to Fe(II) (pathway d in Fig. 4). The indirect reduction of Cr(VI) by biogenic Fe(II) only occurred in the presence of an electron shuttle (pathway d in Fig. 4). Based on the result that the abiotic reduction rate of Cr(VI) by biogenic Fe(II) was 28 times faster than the biotic reduction rate by MR-1, we concluded that the synergistic effect of AQDS and NAu-2/ferrihydrite was attributed to the generated Fe(II) facilitated by AQDS (Pathway d in Fig. 4). This conclusion was further supported by the results that the generated Fe(II) obviously dropped after each spike of Cr(VI)

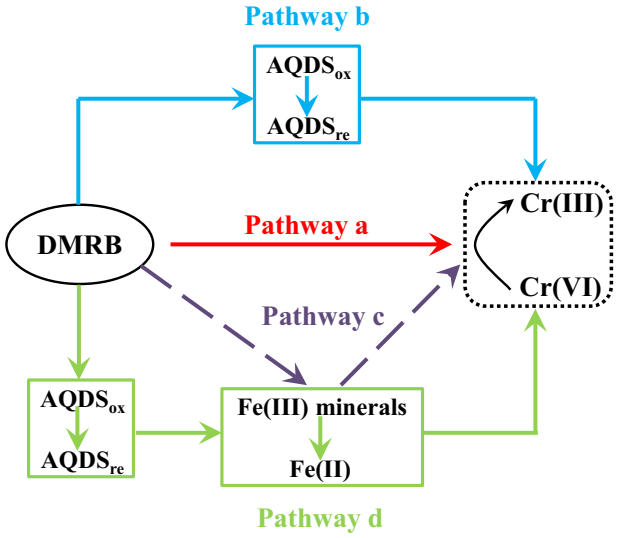

Fig. 4. Possible pathways for the bioreduction of Cr(VI) in the systems containing DMRB, Fe(III) minerals (NAu-2, ferrihydrite and goethite), and AQDS in this study. (a) Direct bioreduction of Cr(VI); (b) indirect reduction of Cr(VI) by bioreduced AQDS; (c) indirect reduction of Cr(VI) by biogenic Fe(II); and (d) indirect reduction of Cr(VI) in the presence of both Fe(III) minerals and AQDS. The dashed arrows represent that the pathway c was proven to be infeasible in this study due to insufficient biogenic Fe(II) in the absence of AQDS.

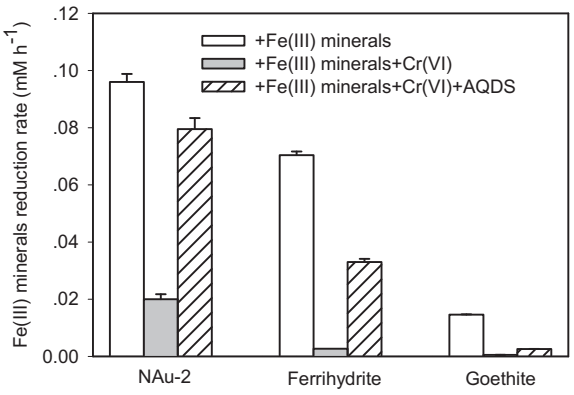

Fig. 5. Zero-order rates for Fe(III) minerals reduction with combinations of MR-1, Cr(VI), and AQDS. Experiments conducted with 7.0×10^8 cells mL^{-1} MR-1, 8.0 mM lactate, 2.0 g L^{-1} iron minerals (NAu-2, ferrihydrite and goethite), with/without Cr(VI) (0.8 mM) and AQDS (0.1 mM) in 30 mM HEPES buffer, pH 7.0.

(Fig. 1e, f and Fig. S3f). Another line of evidence supporting the conclusion was that the synergistic effects increased with the accumulation of generated Fe(II) (Table 3, Spike I to spike III).

Unlike NAu-2 and ferrihydrite, there was no obvious synergistic effect of goethite and AQDS on bioreduction of Cr(VI) (Fig. 2c, Table 3). The bioreduction of iron minerals was affected by some factors, such as Fe(III) species, reduction potentials, crystallization, and surface area (Bird et al., 2011; Wielinga et al., 2001; Xu et al., 2005). In this study, the bioreduction rate of Fe(III) in NAu-2, ferrihydrite, and goethite by MR-1 were 0.096 ± 0.003 mM h^{-1}, 0.070 ± 0.001 mM h^{-1}, and 0.015 ± 0 mM h^{-1}, respectively (Fig. 5), demonstrating that goethite was more difficult to be reduced than NAu-2 and ferrihydrite even in the absence of Cr(VI). Our results were consistent with previous studies which showed that the rate and extent of bioreduction of goethite were considerably less than those of ferrihydrite and iron-bearing clay minerals (Hansel, 2004; Komlos et al., 2007). Although the bioreduction of all three iron minerals was almost fully inhibited by Cr(VI) (Fig. 5), the addition of AQDS facilitated the reduction of NAu-2 and ferrihydrite, where the reduction rate of Fe(III) were 0.079 ± 0.004 mM $h^{-1}$and 0.033 ± 0.001 mM h^{-1}, respectively (Fig. 5). However, even in the presence of AQDS, the reduction of goethite was still almost fully inhibited by Cr(VI), where the reduction rate was only 0.003 ± 0 mM·h^{-1} (Fig. 5). In that case, the generated Fe(II) was <0.1 mM in both spike I and spike II, which was not able to obviously accelerate the reduction of Cr(VI). Therefore, goethite plus AQDS could not synergistically enhance the bioreduction of Cr(VI) by DMRB.

4. Conclusions

We believe this is the first study to report the synergistic effect of iron(III) minerals and electron shuttle on the bioreduction of Cr(VI) by DMRB. Our results show that electron shuttle could facilitate the electron transfer from iron-reducing bacteria to Fe(III) minerals and overcome the inhibition of Fe(III) bioreduction by Cr(VI). Therefore, Fe(III) minerals and electron shuttle synergistically enhance bioreduction of Cr(VI). Our results provide a promising approach to strengthen the bio-immobilization of Cr(VI) at contaminated sites. For example, at iron-rich contaminated sites, the addition of electron shuttles could facilitate the reduction of easily reduced iron minerals (i.e., iron-bearing clay minerals and ferrihydrite) by iron reducing bacteria, which could significantly enhance the immobilization process of Cr(VI). Our results also have important implications for modeling of Cr(VI) reduction kinetics in complex environmental systems containing iron minerals and electron shuttles. Such knowledge is important for better understanding the migration and immobilization of Cr(VI) in the subsurface environment.

Acknowledgements

This research was supported by the National Natural Science Foundation of China (Grant No. 51678557), the 100 Talents Program of Chinese Academy of Sciences, the special fund from Key Laboratory of Drinking Water Science and Technology, Research Center for Eco-Environmental Sciences, Chinese Academy of Sciences (Project No. 15Z09KLDWST), and CPSF-CAS Joint Foundation for Excellent Postdoctoral Fellows (Grant No. 2015LH0037).

Appendix A. Supplementary data

Supplementary data to this article can be found online at https://doi.org/10.1016/j.scitotenv.2018.05.331.

References

Berrodier, I., Farges, F., Benedetti, M., Winterer, M., Brown, G.E., Deveughèle, M., 2004. Adsorption mechanisms of trivalent gold on iron- and aluminum-(oxy)hydroxides. Part 1: X-ray absorption and Raman scattering spectroscopic studies of Au(III) adsorbed on ferrihydrite, goethite, and boehmite. Geochim. Cosmochim. Acta 68, 3019–3042.
Bird, L.J., Bonnefoy, V., Newman, D.K., 2011. Bioenergetic challenges of microbial iron metabolisms. Trends Microbiol. 19, 330–340.
Bishop, M.E., Glasser, P., Dong, H., Arey, B., Kovarik, L., 2014. Reduction and immobilization of hexavalent chromium by microbially reduced Fe-bearing clay minerals. Geochim. Cosmochim. Acta 133, 186–203.
Brookshaw, D.R., Coker, V.S., Lloyd, J.R., Vaughan, D.J., Pattrick, R.A., 2014. Redox interactions between Cr(VI) and Fe(II) in bioreduced biotite and chlorite. Environ. Sci. Technol. 48, 11337–11342.
Buerge, I.J., Hug, S.J., 1997. Kinetics and pH dependence of chromium(VI) reduction by iron(II). Environ. Sci. Technol. 31, 1426–1432.
Butler, E.C., Chen, L., Hansel, C.M., Krumholz, L.R., Elwood Madden, A.S., Lan, Y., 2015. Biological versus mineralogical chromium reduction: potential for reoxidation by manganese oxide. Environ Sci Process Impacts 17, 1930–1940.
Dixit, S., Hering, J.G., 2006. Sorption of Fe(II) and As(III) on goethite in single- and dual-sorbate systems. Chem. Geol. 228, 6–15.
Døssing, L.N., Dideriksen, K., Stipp, S.L.S., Frei, R., 2011. Reduction of hexavalent chromium by ferrous iron: a process of chromium isotope fractionation and its relevance to natural environments. Chem. Geol. 285, 157–166.
Farmer, J.G., Thomas, R.P., Graham, M.C., Geelhoed, J.S., Lumsdon, D.G., Paterson, E., 2002. Chromium speciation and fractionation in ground and surface waters in the vicinity of chromite ore processing residue disposal sites. J. Environ. Monit. 4, 235–243.
Field, E.K., Gerlach, R., Viamajala, S., Jennings, L.K., Peyton, B.M., Apel, W.A., 2013. Hexavalent chromium reduction by Cellulomonas sp. strain ES6: the influence of carbon source, iron minerals, and electron shuttling compounds. Biodegradation 24, 437–450.
Fredrickson, J.K., Kostandarithes, H.M., Li, S.W., Plymale, A.E., Daly, M.J., 2000. Reduction of Fe(III), Cr(VI), U(VI), and Tc(VII) by *Deinococcus radiodurans* R1. Appl. Environ. Microbiol. 66, 2006–2011.
Gonzalez, A.R., Ndung'u, K., Flegal, A.R., 2005. Natural occurrence of hexavalent chromium in the aromas red sands aquifer, California. Environ. Sci. Technol. 39, 5505–5511.
Gorski, C.A., Scherer, M.M., 2011. Fe^{2+} Sorption at the Fe Oxide-water Interface: A Revised Conceptual Framework. Aquatic Redox Chemistry. ACS Publications, pp. 315–343.
Hansel, C.M., 2004. Bacterial and Geochemical Controls on the Reductive Dissolution and Secondary Mineralization of Iron (Hydr) Oxides. Stanford University.
Hori, M., Shozugawa, K., Matsuo, M., 2015. Reduction process of Cr(VI) by Fe(II) and humic acid analyzed using high time resolution XAFS analysis. J. Hazard. Mater. 285, 140–147.
Izbicki, J.A., Bullen, T.D., Martin, P., Schroth, B., 2012. Delta Chromium-53/52 isotopic composition of native and contaminated groundwater, Mojave Desert, USA. Appl. Geochem. 27, 841–853.
Keeling, J.L., Raven, M.D., Gates, W.P., 2000. Geology and characterization of two hydrothermal nontronites from weathered metamorphic rocks at the Uley graphite mine, South Australia. Clay Clay Miner. 48, 537–548.
Komlos, J., Kukkadapu, R.K., Zachara, J.M., Jaffe, P.R., 2007. Biostimulation of iron reduction and subsequent oxidation of sediment containing Fe-silicates and Fe-oxides: effect of redox cycling on Fe(III) bioreduction. Water Res. 41, 2996–3004.
Kukkadapu, R.K., Zachara, J.M., Fredrickson, J.K., McKinley, J.P., Kennedy, D.W., Smith, S.C., et al., 2006. Reductive biotransformation of Fe in shale–limestone saprolite containing Fe(III) oxides and Fe(II)/Fe(III) phyllosilicates. Geochim. Cosmochim. Acta 70, 3662–3676.
Liu, G., Yang, H., Wang, J., Jin, R., Zhou, J., Lv, H., 2010. Enhanced chromate reduction by resting Escherichia coli cells in the presence of quinone redox mediators. Bioresour. Technol. 101, 8127–8131.
Luan, F., Burgos, W.D., 2012. Sequential extraction method for determination of Fe(II/III) and U(IV/VI) in suspensions of iron-bearing phyllosilicates and uranium. Environ. Sci. Technol. 46, 11995–12002.
Luan, F., Burgos, W.D., Xie, L., Zhou, Q., 2010. Bioreduction of nitrobenzene, natural organic matter, and hematite by Shewanella putrefaciens CN32. Environ. Sci. Technol. 44, 184–190.

Luan, F., Gorski, C.A., Burgos, W.D., 2014. Thermodynamic controls on the microbial reduction of iron-bearing nontronite and uranium. Environ. Sci. Technol. 48, 2750–2758.
Luan, F., Liu, Y., Griffin, A.M., Gorski, C.A., Burgos, W.D., 2015. Iron(III)-bearing clay minerals enhance bioreduction of nitrobenzene by Shewanella putrefaciens CN32. Environ. Sci. Technol. 49, 1418–1426.
Mukhopadhyay, B., Sundquist, J., Schmitz, R.J., 2007. Removal of Cr(VI) from Cr-contaminated groundwater through electrochemical addition of Fe(II). J. Environ. Manag. 82, 66–76.
Myers, J.M., Antholine, W.E., Myers, C.R., 2004. Vanadium (V) reduction by Shewanella oneidensis MR-1 requires menaquinone and cytochromes from the cytoplasmic and outer membranes. Appl. Environ. Microbiol. 70, 1405–1412.
Neumann, A., Petit, S., Hofstetter, T.B., 2011. Evaluation of redox-active iron sites in smectites using middle and near infrared spectroscopy. Geochim. Cosmochim. Acta 75, 2336–2355.
Nyman, J.L., Caccavo, F., Cunningham, A.B., Gerlach, R., 2002. Biogeochemical elimination of chromium (VI) from contaminated water. Bioremediation Journal 6, 39–55.
O'Loughlin, E.J., 2008. Effects of electron transfer mediators on the bioreduction of lepidocrocite (gamma-FeOOH) by Shewanella putrefaciens CN32. Environ. Sci. Technol. 42, 6876–6882.
Ona-Nguema, G., Morin, G., Juillot, F., Calas, G., Brown Jr., G.E., 2005. EXAFS analysis of arsenite adsorption onto two-line ferrihydrite, hematite, goethite, and lepidocrocite. Environ. Sci. Technol. 39, 9147–9155.
Panagiotakis, I., Dermatas, D., Vatseris, C., Chrysochoou, M., Papassiopi, N., Xenidis, A., et al., 2015. Forensic investigation of a chromium(VI) groundwater plume in Thiva, Greece. J. Hazard. Mater. 281, 27–34.
Pettine, M., D'Ottone, L., Campanella, L., Millero, F.J., Passino, R., 1998. The reduction of chromium (VI) by iron (II) in aqueous solutions. Geochim. Cosmochim. Acta 62, 1509–1519.
Saha, R., Nandi, R., Saha, B., 2011. Sources and toxicity of hexavalent chromium. J. Coord. Chem. 64, 1782–1806.
Sani, R.K., Peyton, B.M., Dohnalkova, A., 2008. Comparison of uranium (VI) removal by Shewanella oneidensis MR-1 in flow and batch reactors. Water Res. 42, 2993–3002.
Sathishkumar, K., Murugan, K., Benelli, G., Higuchi, A., Rajasekar, A., 2017. Bioreduction of hexavalent chromium by pseudomonas stutzeri L1 and Acinetobacter baumannii L2. Ann. Microbiol. 67, 91–98.
Schwertmann, U., Cornell, R.M., 2008. Iron Oxides in the Laboratory: Preparation and Characterization. John Wiley & Sons.
Sedlak, D.L., Chan, P.G., 1997. Reduction of hexavalent chromium by ferrous iron. Geochim. Cosmochim. Acta 61, 2185–2192.
Tahri Joutey, N., Bahafid, W., Sayel, H., Ananou, S., El Ghachtouli, N., 2014. Hexavalent chromium removal by a novel Serratia proteamaculans isolated from the bank of Sebou River (Morocco). Environ. Sci. Pollut. Res. Int. 21, 3060–3072.
Viamajala, S., Peyton, B.M., Petersen, J.N., 2003. Modeling chromate reduction in Shewanella oneidensis MR-1: development of a novel dual-enzyme kinetic model. Biotechnol. Bioeng. 83, 790–797.
Weng, C.-H., Lin, Y.-T., Yuan, H.-M., 2013. Rapid decoloration of reactive black 5 by an advanced Fenton process in conjunction with ultrasound. Sep. Purif. Technol. 117, 75–82.
Wielinga, B., Mizuba, M.M., Hansel, C.M., Fendorf, S., 2001. Iron promoted reduction of chromate by dissimilatory iron-reducing bacteria. Environ. Sci. Technol. 35, 522–527.
Wikipedia, 2017. https://en.wikipedia.org/wiki/Synergy, Accessed date: 10 December 2017.
Xu, W., Liu, Y., Zeng, G., Li, X., Tang, C., Yuan, X., 2005. Enhancing effect of iron on chromate reduction by Cellulomonas flavigena. J. Hazard. Mater. 126, 17–22.
Zheng, Z., Li, Y., Zhang, X., Liu, P., Ren, J., Wu, G., et al., 2015. A *Bacillus subtilis* strain can reduce hexavalent chromium to trivalent and an nfrA gene is involved. Int. Biodeterior. Biodegrad. 97, 90–96.
Zhou, T., Lim, T.T., Wu, X., 2011. Sonophotolytic degradation of azo dye reactive black 5 in an ultrasound/UV/ferric system and the roles of different organic ligands. Water Res. 45, 2915–2924.
Zhou, T., Wu, X., Zhang, Y., Li, J., Lim, T.-T., 2013. Synergistic catalytic degradation of antibiotic sulfamethazine in a heterogeneous sonophotolytic goethite/oxalate Fenton-like system. Appl. Catal. B Environ. 136-137, 294–301.